Journal of Zhejiang University-SCIENCE A (Applied Physics & Engineering)
ISSN 1673-565X (Print); ISSN 1862-1775 (Online)
www.zju.edu.cn/jzus; www.springerlink.com
E-mail: jzus@zju.edu.cn

Investigation of low-cycle fatigue behavior of austenitic stainless steel for cold-stretched pressure vessels*

Cun-jian MIAO, Jin-yang ZHENG†‡, Xiao-zhe GAO, Ze HUANG, A-bin GUO, Du-yi YE, Li MA

(*Institute of Process Equipment, Zhejiang University, Hangzhou 310027, China*)

†E-mail: jyzh@zju.edu.cn

Received June 5, 2012; Revision accepted Nov. 8, 2012; Crosschecked Dec. 10, 2012

Abstract: Cold-stretched pressure vessels from austenitic stainless steels (ASS) are widely used for storage and transportation of liquefied gases, and have such advantages as thin wall and light weight. Fatigue is an important concern in these pressure vessels, which are subjected to alternative loads. Even though several codes and standards have guidelines on these pressure vessels, there are no relevant design methods on fatigue failure. To understand the fatigue properties of ASS 1.4301 (equivalents include UNS S30400 and AISI 304) in solution-annealed (SA) and cold-stretched conditions (9% strain level) and the response of fatigue properties to cold stretching (CS), low-cycle fatigue (LCF) tests were performed at room temperature, with total strain amplitudes ranging from ±0.4% to ±0.8%. Martensite transformations were measured during the tests. Comparisons on cyclic stress response, cyclic stress-strain behavior, and fatigue life were carried out between SA and CS materials. Results show that CS reduces the initial hardening stage, but prolongs the softening period in the cyclic stress response. Martensite transformation helps form a stable regime and subsequent secondary hardening. The stresses of monotonic and cyclic stress-strain curves are improved by CS, which leads to a lower plastic strain and a much higher elastic strain. The fatigue resistance of the CS material is better than that of the SA material, which is approximately 1×10^3 to 2×10^4 cycles. The S-N curve of the ASME standard for ASS is compared with the fatigue data and is justified to be suitable for the fatigue design of cold-stretched pressure vessels. However, considering the CS material has a better fatigue resistance, the S-N curve will be more conservative. The present study would be helpful in making full use of the advantages of CS to develop a new S-N curve for fatigue design of cold-stretched pressure vessels.

Key words: Cold stretching (CS), Austenitic stainless steel (ASS), Pressure vessels, Low-cycle fatigue (LCF), Cyclic stress response (CSR), Fatigue life, S-N curve

doi:10.1631/jzus.A1200140 **Document code:** A **CLC number:** TH49

1 Introduction

Austenitic stainless steels (ASS), which are always used as shells of pressure vessels to store and transport liquefied gases, have good ductility and corrosion resistance. Compared with conventional pressure vessels, cold-stretched pressure vessels have such advantages as thin wall (approximately 50% to 70% of the conventional ones with the same pressure parameters), light weight, low cost, and low energy consumption. Several codes and standards for cold-stretched pressure vessels from ASS have been established, such as AS 1210 Supplement 2 (1999), EN 13458-2 (2002), EN 13530-2 (2002), ISO 20421-1 (2006), ISO 21009-1 (2008), and ASME Boiler & Pressure Vessel Code (BPVC) VIII-1 Appendix (2011). Fatigue is an important concern for pressure vessels that are subjected to alternative loads. So far, there are no fatigue design guidelines for cold-stretched pressure vessels in the above corresponding standards. To help develop a favorable fatigue design method for cold-stretched pressure vessels, fatigue properties of ASS that respond to cold stretching (CS, which is also called work hardening,

‡ Corresponding author

* Project supported by the National Key Technology R&D Program (No. 2011BAK06B02-05), the International Science and Technology Cooperation Project (No. 2010DFB42960), and the Key Technology Innovation Team of Zhejiang Province (No. 2010R50001), China

cold working, pre-straining, or preloading) need to be understood.

Investigations of the effects of CS on ASS fatigue behaviors have been carried out at different temperatures, CS levels, CS methods, and specimens' cross sections (Zeedijk, 1977; Rao *et al*., 1993; Bergengren *et al*., 1995; Ganesh Sundara Raman and Padmanabhan, 1996; Johansson and Nordberg, 2002; Hong *et al*., 2003; Hong, 2004; Hong and Lee, 2004; Srinivasan *et al*., 2004; Nakajima *et al*., 2010; 2011). After CS, better fatigue resistances have been reported at different strain amplitudes. Martensite transformations have been detected during cycling, making an important contribution to fatigue properties. Fatigue behaviors, such as cyclic stress response and cyclic stress-strain curve, have been described and analyzed, but little was mentioned about fatigue design methods for pressure vessels, such as the S-N curves. Different temperatures, CS levels, and CS methods lead to different fatigue behaviors and results. For cold-stretched pressure vessels in China, a 9% CS level is commonly employed and carried out by CS parallel to the rolling direction at room temperature. Dog bone-shaped specimens are usually used in fatigue tests. These are not covered by prior research. In addition, fatigue design S-N curves are very concerned for pressure vessels.

This study focuses on cold-stretched pressure vessels in China. Detailed research was performed on a commercial industrial ASS material grade EN 1.4301 (equivalents include UNS S30400, AISI 304) in solution-annealed (SA) and CS conditions. The 9% CS level is introduced on the ASS material by tension. Dog bone-shaped specimens are used to perform fatigue tests. Low-cycle fatigue (LCF) properties responding to the 9% CS level at room temperature are studied. Cyclic stress response (CSR), cyclic stress-strain curve (CSSC), and fatigue life are exhibited to reveal the effect of CS. These fatigue data are compared with the S-N curve of ASME standards.

2 Experimental

2.1 Test material

A commercial industrial ASS grade EN 1.4301 was selected for this investigation. It was delivered in the form of a 16 mm-thick plate under a hot-rolled and SA condition. Its chemical composition is shown in Table 1. The samples with dimensions of 16 mm× 16 mm×200 mm were machined from the plates and then cold-stretched to a 9% total strain, with the longitudinal axis parallel to the rolling direction. CS was carried out with a quasi-static rate of 1×10^{-4} s^{-1}. Then, the dog bone-shaped specimens with a gauge diameter of 6 mm and a gauge length of 12 mm were fabricated for both SA and CS conditions. To compare with previous results (Zeedijk, 1977; Rao *et al.*, 1993), M_{D30} was calculated and listed in Table 1, where M_{D30} is the temperature at which 50% (in volume) strain-induced martensite transformation will occur in material after 30% stretching. Note that the ASS shows a higher M_{d30}, which means that the ASS is more unstable and is likely to generate more martensite.

2.2 Low-cycle fatigue and tensile tests

LCF tests were conducted in air under a fully reversed and total axial strain control in an MTS 810 servo-hydraulic testing machine. A symmetrical, triangular strain-time wave form was used. These tests were performed at room temperature based on the test standard ASTM E606, with strain amplitudes ranging from ±0.4% to ±0.8% at a constant strain rate of 4×10^{-3} s^{-1}. The tensile tests were carried out in the same machine with the same strain rate. Strain was detected using an MTS extensometer.

2.3 Martensite transformation

The α'-martensite transformation of ASS is considered to be an important factor in a material's mechanical behavior, which should be detected during tests. Some methods, such as ferrite-scope

Table 1 Chemical composition and M_{D30} of the tested material

Study	M_{D30} (°C)	Chemical composition (%, in weight)							
		C	Si	Mn	P	S	Cr	Ni	N
This study	7	0.020	0.38	1.77	0.029	0.001	18.29	8.05	0.068
Zeedijk, 1977	−42	0.045	0.30	1.20	–	–	17.50	11.00	–
Rao *et al*., 1993	−3	0.042	0.38	1.65	0.024	0.003	18.20	9.20	–

measurement and metallographic examination, are commonly used to measure martensite transformation. Compared with metallographic examination, which can qualitatively prove the existence of the martensite phase with destruction of the material, ferrite-scope measurement, as a non-destructive method, can make a quantitative detection at different stages during cycling. Further, based on the comparison (Talonen *et al*., 2004), the ferrite-scope method was the easiest way of measuring the content of martensite transformation.

The variation in martensite transformation during cycling was observed. The ferrite-scope (model FMP30, Helmut Fischer GmbH +Co., Germany) was employed to measure the content of transformation. The results were presented by ferrite number (FN).

3 Results

3.1 Cyclic stress response (CSR) and martensite transformation

The CSR curves of SA and CS conditions are illustrated in Fig. 1. As shown in Fig. 1a, the CSR of the SA material exhibits a relatively long period of cyclic hardening and reaches a maximum stress value at an early stage (within 5 to 20 cycles). After cyclic hardening, a prolonged softening regime is observed. A short stable stress response follows, and then a strong secondary hardening stage appears. Finally, failure happens. Compared with the CSR of the SA material, the CSR of the CS material shows a similar response, but has a shorter period of initial hardening and a longer softening regime. The stress responses of both SA and CS materials improve with an increase in strain amplitudes. Fig. 1 shows that the CSR in CS 1.4301 are higher than that displayed by the SA material at the same strain amplitudes.

The cyclic martensite transformations of both the SA and CS materials are described by FN in Fig. 2. The transformations of both the SA and CS materials consist of two stages. First, there is a stable regime when cyclic martensite varies slightly during cycling. Then, an obvious acceleration of martensite transformation takes place at a specific cycle, which is dependent on strain amplitudes. Furthermore, acceleration occurs earlier at higher strain amplitude. Fig. 2 shows that the martensite contents generated in the SA and CS materials are nearly the same at low strain amplitudes. As strain amplitude increases, transformation is faster in the CS material than that in the SA material.

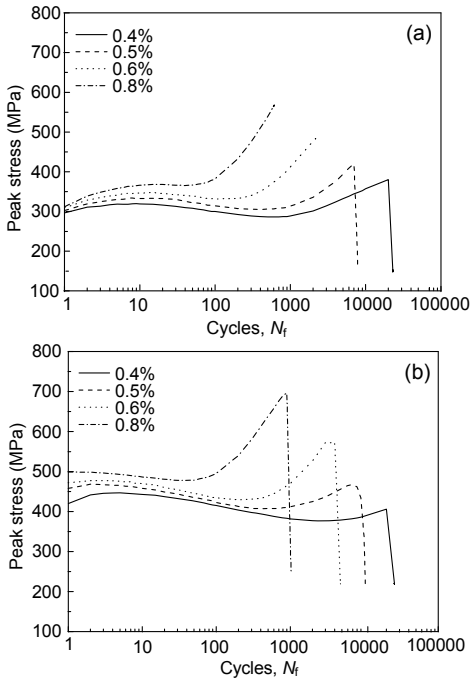

Fig. 1 Effect of strain amplitude on the CSR of SA 1.4301 (a) and CS 1.4301 (b)

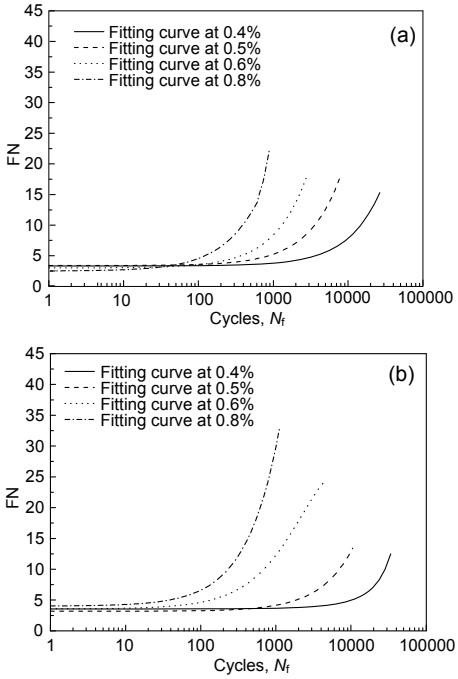

Fig. 2 Effect of strain amplitude on the cyclic martensite content (FN) of SA 1.4301 (a) and CS 1.4301 (b)

3.2 Monotonic and cyclic stress-strain curves

Table 2 shows the tensile properties of ASS 1.4301 in SA and CS conditions at room temperature. These properties reveal that both yield strength (YS) and ultimate tensile strength (UTS) increase after CS. The increase of UTS is much lower than that of YS. Ductility (percentage elongation to fracture) decreases after CS, whereas reduction in area (RA) and true fracture strain ε_f (deduced by RA) exhibit a slight increase. A similar increase in YS and UTS was also reported in other research (Rao *et al*., 1993; Hong *et al*., 2003), which was mainly attributed to strain-induced martansite during CS.

Fig. 3 shows both monotonic stress-strain curve (MSSC) and CSSC of the SA and CS materials. CS is conducted in the tensile tests, leading to high stresses in the MSSC of the CS material. Both MSSC and CSSC are raised by CS to a higher level, although the stress difference between SA and CS conditions in CSSC is reduced compared with that of MSSC, which has suggested (Rao *et al*., 1993) that the effect of strengthening in monotonic strength properties induced by CS could not be retained fully under fatigue conditions.

3.3 Fatigue life

Table 3 summarizes the effect of strain amplitude and CS on LCF parameters. The values of total strain amplitude ($\Delta\varepsilon_t/2$), plastic strain amplitude ($\Delta\varepsilon_p/2$), elastic strain amplitude ($\Delta\varepsilon_e/2$), and the number of cycles to failure (N_f) are included, as well as the peak stress of the first cycle $(\Delta\sigma/2)_1$ and the stress amplitude for the cycle corresponding to half the failure life ($\Delta\sigma/2$). Fatigue life N_f is defined as the number of cycles corresponding to a 25% drop in stress amplitude ($\Delta\sigma/2$) or cycles to failure, and the difference between them is negligible (O'Donnell and O'Donnell, 2005).

The variation in fatigue life, with total, plastic, and elastic strain amplitudes in SA and CS conditions, is shown in Fig. 4. It shows that CS improves fatigue resistance in a strain range of ±0.4% to ±0.8%. Similar effects of CS on fatigue life were reported (Rao *et al.*, 1993; Bergengren *et al*., 1995; Ganesh Sundara Raman and Padmanabhan, 1996; Johansson and Nordberg, 2002). Transition fatigue life is determined by the intersection between $\Delta\varepsilon_p/2$–N_f and $\Delta\varepsilon_e/2$–N_f curves, and is shorter in CS condition than in SA condition.

Table 3 LCF properties of both SA and CS materials at room temperature

Condition	$\Delta\varepsilon_t/2$ (%)	$\Delta\varepsilon_e/2$ (%)	$\Delta\varepsilon_p/2$ (%)	$(\Delta\sigma/2)_1$ (MPa)	$(\Delta\sigma/2)$ (MPa)	N_f
SA	0.4	0.233	0.168	296	361	22962
	0.5	0.232	0.268	302	375	7826
	0.6	0.233	0.367	320	424	2172
	0.8	0.314	0.486	312	478	616
CS	0.4	0.260	0.140	391	406	25574
	0.5	0.301	0.199	422	475	10333
	0.6	0.313	0.287	452	558	4781
	0.8	0.364	0.436	471	650	1031

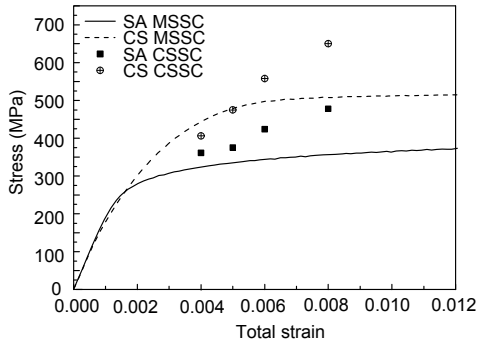

Fig. 3 Cyclic stress-strain curves and monotonic stress-strain curves of SA and CS materials

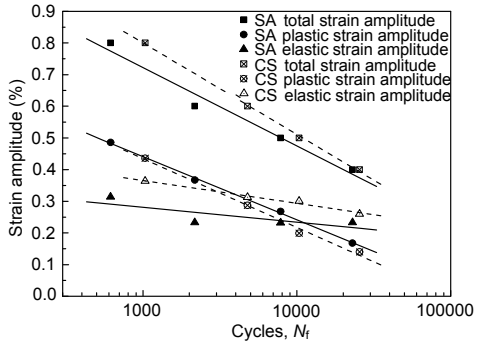

Fig. 4 Strain-life plots of ASS 1.4301 in SA and CS conditions

Table 2 Tensile properties of ASS 1.4301 in SA and CS conditions at room temperature

Condition	YS (MPa)	UTS (MPa)	Elongation to fracture (%)	RA (%)	$\varepsilon_f = \ln\frac{1}{1-\mathrm{RA}}$
SA	318	702	77.5	78.4	1.53
CS	461	757	71.5	80.0	1.61

4 Discussion

4.1 Effect of CS on cyclic stress response

Fig. 5 shows the comparison between the CSR of SA and CS materials at ±0.5% strain amplitude, with a corresponding cyclic martensite transformation. The CSR of both materials comprises four stages, namely, initial hardening, softening, saturation (the stable regime), and secondary hardening. Cyclic softening is pronounced in the whole stress response and was reported earlier (Rao *et al*., 1993). Cyclic softening is considered as a recovery process induced by cyclic strain, which leads to low energy dislocation structures characterized by cells and sub-grains (Laird *et al*., 1989). The softening of cold-worked materials and those having high initial dislocation densities occurs when the annihilation rate of dislocation is greater than the generation rate, causing a net decrease in dislocation densities, or when the rearrangement of the dislocations takes place into cellular structure, resulting in an increase in the mean free path for dislocations (Feltner and Beardmore, 1970). This explanation can also account for the observed softening at present.

Fig. 5 shows that as martensite content begins to grow quickly, softening begins to disappear, and a stable response happens. After a short stable response, the secondary hardening occurs. All these cyclic stress responses could be attributed to the increase in martensite content (Ganesh Sundara Raman and Padmanabhan, 1996). The existence of the secondary hardening stage is different from previous studies (Zeedijk, 1977; Rao *et al*., 1993), where no secondary hardening occurred and the specimen failed after the stable stage in the SA material. Based on M_{D30} in Table 1, the proposed ASS generates more martensite transformation, which may cause the secondary hardening stage. ASS with lower M_{D30} is more stable and may not lead to the secondary hardening in the end.

CS is found to affect the CSR to some extent. In Fig. 5, at ±0.5% strain amplitude, CS decreases the range of the initial hardening and the secondary hardening, and lengthens the softening process. However, CS still improves the whole stress response. Higher pre-deformation levels could lead to cyclic softening beginning with the first cycle and onward, whereas lower pre-deformation levels could cause initial hardening prior to softening (Srinivasan *et al.*, 2004). This could also be proven by comparing the CSRs of the SA and the CS at ±0.8% strain amplitude. Furthermore, CS appears to delay the secondary hardening.

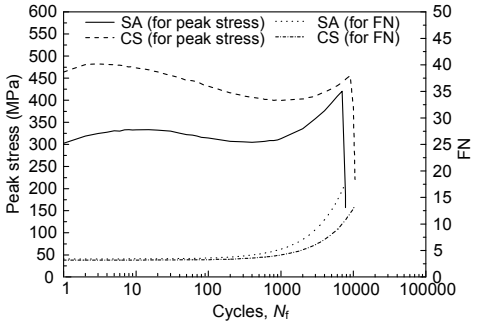

Fig. 5 Effect of CS on CSR and cyclic martensite transformation at ±0.5% strain amplitude

4.2 Effect of CS on stress-strain curves

In Table 2 and Fig. 3, CS increases the strength of both the MSSC and the CSSC curves. The strength increment of CSSC is smaller than that of MSSC. Owing to the work-hardening effect of CS, a higher strength and a lower plastic strain were produced during cycling, which imply a lower plastic strain concentration and a higher elastic strain range during fatigue cycles. This may help improve fatigue resistance.

4.3 Effect of CS on fatigue life

Rao *et al*. (1993) found that CS reduced total strain fatigue resistance at large strains, with 304 at room temperature, but seemed to improve resistance beyond 2×10^4 reversals (at about ±0.3%). Bergengren *et al*. (1995) found that CS made resistance better after about 1×10^4 cycles (at about ±0.35%) for 304. Johansson and Nordberg (2002) found that fatigue life was better between approximately 7×10^3 and 1×10^6 cycles for 1.4301. These are different from the results of this study, which indicates that fatigue resistance is better in CS condition than in SA in the range of 1×10^3 to 2×10^4 cycles (from ±0.4% to ±0.8% strain amplitudes). This difference, as well as that in the CSRs, may be caused by the difference in the factors mentioned before, such as specimens' cross sections, CS levels, and CS methods. In addition, the chemical composition and the manufacturing technology of ASS may also have effects on that.

Fatigue life is known generally to be governed by the ductility of a material at high strain amplitudes and by its strength at low strain amplitudes (Feltner and Beardmore, 1970; Rao *et al*., 1993; Ganesh Sundara Raman and Padmanabhan, 1996). Some of the capacity of the material to deform plastically is consumed by CS, which leads to a higher CSSC and could cause lower plastic and higher elastic amplitudes in the CS material. Fig. 4 shows that the CS material exhibits greater fatigue resistance at all strain amplitudes than the SA material when the comparison is made on the basis of elastic strain amplitude. However, an opposite conclusion is drawn when the comparison is made based on plastic strain amplitude. At low strain amplitudes, the results in this investigation are similar with those in the studies mentioned above, which showed the importance of strength. At high strain amplitudes, both SA and CS fatigue resistance of plastic strain amplitude are nearly the same. Therefore, it is suggested that the longer life of the CS material may be caused by the much larger resistance of elastic strain amplitudes at high strain amplitudes.

4.4 S-N curves

The measured fatigue data are compared with the ASME BPVC VIII-2 (2010) fatigue S-N design curve for ASS materials in Fig. 6. Both SA and CS materials' fatigue data are above the ASME S-N curve, which indicates that the ASME S-N curve could be used for the fatigue design of cold-stretched vessels. Considering that the CS material has a better fatigue resistance, the ASME S-N curve that is always used for SA materials will be more conservative for cold-stretched vessels, and a new S-N curve is suggested to make full use of the advantages of CS.

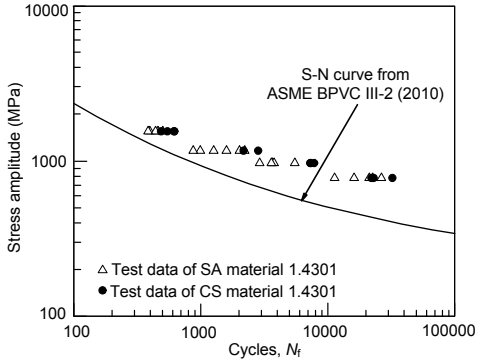

Fig. 6 Comparison between the measured fatigue data of ASS 1.4301 and the S-N curve of ASME BPVC VIII-2 (2010)

5 Conclusions

Based on the tensile test results, LCF tests and martensite content measurement for ASS EN 1.4301 in SA and CS conditions, as well as the effects of CS on fatigue properties, are discussed. The following conclusions are made:

1. CSR shows the same behavior, which is characterized by initial hardening followed by softening, stable period, and then secondary hardening, in both SA and CS conditions. CS makes the CSR higher and gives a shorter initial hardening stage and a longer softening stage. When martensite content begins to grow fast, it has a strong effect on CSR, which leads to a stable period and a subsequent secondary hardening. CS is also responsible for a later beginning of the stable stage.

2. CS improves the strength of MSSC. This strength improvement is retained, but is reduced in the CSSC. This may lead to a lower plastic strain response and a weaker plastic strain concentration during cycling, and help improve fatigue resistance.

3. CS decreases transition life, but enhances fatigue resistance from approximately 1×10^3 to 2×10^4 cycles (between strain amplitudes from ±0.4% to ±0.8%). The higher life of the CS material at high strain amplitudes may be caused by a much higher resistance of elastic strain amplitudes. The ASME S-N curve for ASS is justified to be suitable for the fatigue design of cold-stretched pressure vessels. The present study would be helpful in making full use of the advantages of CS in developing the fatigue design of cold-stretched pressure vessels.

References

AS 1210 Supplement 2, 1999. Pressure Vessels-Cold-Stretched Austenitic Stainless Steel Vessels. Standards Association of Australia.

ASME Boiler & Pressure Vessel Code (BPVC) VIII-1 Appendix, 2011. Cold-Stretching of Austenitic Stainless Steel Pressure Vessels. The American Society of Mechanical Engineers.

ASME Boiler & Pressure Vessel Code (BPVC), VIII-2, 2010. Rules for Construction of Pressure Vessels. The American Society of Mechanical Engineers.

Bergengren, Y., Larsson, M., Melander, A., 1995. Fatigue properties of stainless sheet steels in air at room temperature. *Materials Science and Technology*, **11**(12): 1275-1280. [doi:10.1179/026708395790164562]

EN 13458-2, 2002. Cryogenic Vessels-Static Vacuum Insulated Vessels Part 2: Design, Fabrication, Inspection

and Testing. European Committee for Standardization.

EN 13530-2, 2002. Cryogenic Vessels-Large Transportable Vacuum Insulated Vessels Part 2: Design, Fabrication, Inspection and Testing. European Committee for Standardization.

Feltner, C.E., Beardmore, P., 1970. Strengthening Mechanisms in Fatigue. ASTM, Philadelphia, PA, USA, p.77-112.

Ganesh Sundara Raman, S., Padmanabhan, K.A., 1996. Effect of prior cold work on the room-temperature low-cycle fatigue behaviour of AISI 304LN stainless steel. *International Journal of Fatigue*, **18**(2):71-79. [doi:10.1016/0142-1123(95)00078-X]

Hong, S.G., 2004. The tensile and low-cycle fatigue behavior of cold worked 316L stainless steel: influence of dynamic strain aging. *International Journal of Fatigue*, **26**(8):899-910. [doi:10.1016/j.ijfatigue.2003.12.002]

Hong, S.G., Lee, S.B., 2004. Dynamic strain aging under tensile and LCF loading conditions, and their comparison in cold worked 316L stainless steel. *Journal of Nuclear Materials*, **328**(2-3):232-242. [doi:10.1016/j.jnucmat.2004.04.331]

Hong, S.G., Yoon, S., Lee, S.B., 2003. The effect of temperature on low-cycle fatigue behavior of prior cold worked 316L stainless steel. *International Journal of Fatigue*, **25**(9-11):1293-1300. [doi:10.1016/s0142-1123(03)00154-3]

ISO 20421-1, 2006. Cryogenic Vessels-Large Transportable Vacuum-Insulated Vessels-Part 1-Design, Fabrication, Inspection and Testing. International Standardization Organization.

ISO 21009-1, 2008. Cryogenic Vessels-Static Vacuum-Insulated Vessels-Part 1-Design, Fabrication, Inspection and Tests. International Standardization Organization.

Johansson, R., Nordberg, H., 2002. Fatigue Properties of Stainless Steel Strip. AvestaPolarit R&D.

Laird, C., Wang, Z., Ma, B.T., Chai, H.F., 1989. Low energy dislocation structures produced by cyclic softening. *Materials Science and Engineering*: *A*, **113**(1):245-257. [doi:10.1016/0921-5093(89)90313-4]

Nakajima, M., Akita, M., Uematsu, Y., Tokaji, K., 2010. Effect of strain-induced martensitic transformation on fatigue behavior of type 304 stainless steel. *Procedia Engineering*, **2**(1):323-330. [doi:10.1016/j.proeng.2010.03.036]

Nakajima, M., Uematsu, Y., Kakiuchib, T., Akita, M., Tokaji, K., 2011. Effect of quantity of martensitic transformation on fatigue behavior in type 304 stainless steel. *Procedia Engineering*, **10**:299-304. [doi:10.1016/j.proeng.2011.04.052]

O'Donnell, W.J., O'Donnell, T.P., 2005. Proposed New Fatigue Design Curves for Austenitic Stainless Steels, Alloy 600 and Alloy 800. Proceedings of the ASME Pressure Vessels and Piping Conference, Denver, CO. ASME, USA, **1**:109-132. [doi:10.1115/PVP2005-71409]

Rao, K.B.S., Valsan, M., Sandhya, R., Mannan, S.L., Rodriguez, P., 1993. An assessment of cold work effects on strain-controlled low-cycle fatigue behavior of type-304 stainless-steel. *Metallurgical Transactions A-Physical Metallurgy and Materials Science*, **24**(4):913-924. [doi:10.1007/BF02656512]

Srinivasan, V.S., Sandhya, R., Valsan, M., Rao, K.B.S., Mannan, S.L., 2004. Comparative evaluation of strain controlled low cycle fatigue behaviour of solution annealed and prior cold worked 316L(N) stainless steel. *International Journal of Fatigue*, **26**(12):1295-1302. [doi:10.1016/j.ijfatigue.2004.5.003]

Talonen, J., Aspegren, P., Hanninen, H., 2004. Comparison of different methods for measuring strain induced alpha'-martensite content in austenitic steels. *Materials Science and Technology*, **20**(12):1506-1512. [doi:10.1179/026708304x4367]

Zeedijk, H.B., 1977. Cyclic hardening and softening of annealed and 9%-prestrained AISI 304 stainless steel during high strain cycling at room temperature. *Metal Science*, **11**(5):171-176.